

Primljen / Received: 19.12.2020.

Ispravljen / Corrected: 10.11.2021.

Prihvaćen / Accepted: 19.12.2021.

Dostupno online / Available online: 10.9.2022.

# Assessment of fragility curve for steel frame construction under different categories of earthquakes

## Autori:



<sup>1</sup>Assist.Prof. **Huihui Zhao**  
zhaohuihui2020@126.com  
Corresponding author



<sup>2</sup>**Xiaopeng Wang**  
zcgstd@126.com



<sup>3</sup>**Zhichun Fang**  
fzc@stdu.edu.cn



<sup>4</sup>**Siqi Wu**  
Wusiqi20210525@163.com



<sup>5</sup>**Mansour Afzal**, MCE  
Masour.A@hotmail.com

Professional paper

**Huihui Zhao, Xiaopeng Wang, Zhichun Fang, Siqi Wu, Mansour Afzal**

## Assessment of fragility curve for steel frame construction under different categories of earthquakes

The aim of this study is to investigate the effect of two categories of earthquake events on the fragility curves of steel building construction (structures with different number of stories) by considering relative lateral displacement as a damage criterion. The categories used to describe the change in the relative lateral position were chosen to be slight, moderate, extensive, and complete. Increased seismic demand increases the probability of exceeding. In other words, the greater the maximum earthquake acceleration, the higher is the probability of exceeding (PoE). In a 3-story structure, the increase in PGA increases the PoE of the structure at extensive failure levels. The fragility curves for the 2nd category earthquakes show a shift from the sleeping mode (gradual increase) to the standing state (rapid increase) compared to the 1st-class earthquakes in the 5-story model. Increasing the number of stories increases the PoE of extensive and large failures. The PoE of the extensive mode in the 7-story model was 10 and 15.5 % higher than that in the 5- and 3-story models, respectively. However, for the complete damage state, the PoE in the 5-story model was 6 and 7 % more than that in the 7- and 3-story models, respectively. Therefore, it can be concluded that increasing the number of stories increases the PoE, but this increase is more evident for the extensive failure level.

### Key words:

fragility curve, steel structure, probability of exceeding, incremental dynamic analysis (IDA)

Stručni rad

**Huihui Zhao, Xiaopeng Wang, Zhichun Fang, Siqi Wu, Mansour Afzal**

## Procjena krivulje oštetljivosti čelične okvirne konstrukcije kod različitih potresa

Cilj je ovog istraživanja ispitati učinak dviju kategorija potresnih događaja na krivulju oštetljivosti čelične okvirne konstrukcije zgrade (građevine s različitim brojem katova) razmatranjem relativnog bočnog pomaka kao kriterija oštećenosti. Kategorije za opisivanje promjene relativnog bočnog položaja bile su blaga, umjerena, značajna i potpuna. Kako se povećava seizmički zahtjev, veća je vjerojatnost prekoračenja. Drugim riječima, ako maksimalno ubrzanje potresa raste, povećava se vjerojatnost prekoračenja (eng. probability of exceeding - PoE). Povećanja vršnog ubrzanja tla (PGA) povećat će PoE trokatne konstrukcije pri značajnom oštećenju. Krivulje oštetljivosti druge kategorije pokazuju pomak iz stanja mirovanja (postupni porast) u stanje stajanja (nagli porast) u usporedbi s potresima prve klase kod modela s pet katova. Sve veći broj katova utječe na povećanje PoE pri značajnom i teškom oštećenju i povećava vjerojatnost prekoračenja. Model sa sedam katova u značajnom načinu ima 10 i 15,5 % PoE veći od modela s pet i tri kata. Međutim, u stanju potpune oštećenosti, PoE u modelu s pet katova je 6 i 7 puta veća nego u modelu sa sedam i tri kata. Stoga se može zaključiti da je s povećanjem broja katova porasala PoE, što se može bolje uočiti pri značajnom stupnju oštećenja.

### Ključne riječi:

krivulje oštetljivosti, čelične konstrukcije, vjerojatnost prekoračenja, inkrementalna dinamička analiza (IDA)

<sup>1</sup> Yuncheng Vocational and Technical University, Yuncheng, China  
Department of Architecture and Civil Engineering

<sup>2</sup> Shanxi Yuncheng Construction Engineering Group, China

<sup>3</sup> Shijiazhuang Tiedao University, Shijiazhuang, China  
School of Civil Engineering

<sup>4</sup> Shijiazhuang Tiedao University, Shijiazhuang, China  
School of Traffic and Transportation

<sup>5</sup> Islamic Azad University, Ardabil, Iran

## 1. Introduction

General construction requirements from the perspective of earthquake risk management, human protection, structural behavior, and manufacturing safety have been studied [1, 2]. One of the main strategies in earthquake risk management is risk mitigation, which includes the goal of decreasing the seismic vulnerability of impacted structures. As a result, incorporating seismic rehabilitation guidelines necessitates specialists and engineers to consider seismic criteria in their designs [3–5]. One important step in predicting structural behavior before an earthquake is identifying the strengths and weaknesses of structures [6, 7].

In this direction, the use of fragility curves (FRC) before and after an earthquake has been proposed [8]. To analyze various structures statistically using probability theory, the correlation between earthquake intensity and the vulnerability of structures has been investigated in a statistical format [9]. It is important from two perspectives:

- Given a statistically significant correlation between the magnitude of the earthquake and the considerable earthquake damage, the consequences of future earthquakes can be predicted.
- By recognizing further flaws in the design of structures, it is possible to improve additional seismic codes and enhance the safety of structures [10].

The FRC expresses the probability of a breakdown corresponding to a specific damage state at several ground seismic movement levels. In fact, the FRC describes the possible seismic severity ratio between the seismic intensity and the level of seismic breakdown [11].

As part of the Global Earthquake Model (GEM), the OpenQuake-platform has published hundreds of experimental and detailed vulnerability and fragility functions [12, 13]. There are many regions in the world where vulnerability and fragility function models are not easily accessible, despite their increased availability in recent decades, as illustrated in Figure 1.

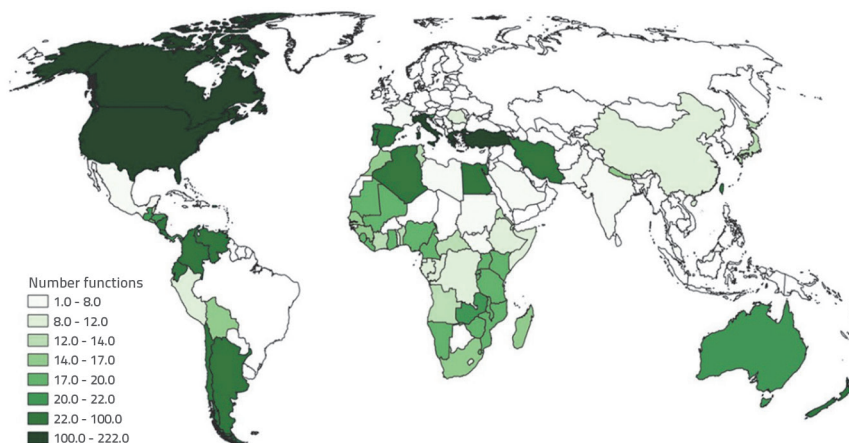


Figure 1. Number of fragility or vulnerability functions per country in the OpenQuake-platform

To accurately determine the FRCs, the correct choice of earthquake intensity in the structure region is an effective parameter [14, 15]. Some of the indicators that identify the severity of the earthquake suitable for fragility analysis are the maximum ground acceleration (PGA) [16], maximum ground velocity (PGV) [17], and maximum ground displacement (PGD) [18]. These fragility curves can be obtained from a rational regression analysis of the actual or simulated damage data or using numerical methods [19]. In the last two decades, FRCs have been widely used by the scientific community for assessing structural behavior and the risk caused by earthquakes [20, 21]. The failure curve method has significant advantages. The method uses a simple approach; its value is an indicator of the vulnerability of the structure and its components, and the expected damage surface can be estimated for a given earthquake intensity [22].

The primary step in seismic risk assessment is estimating the physical damage to the components of infrastructure following a seismic event [23]. The FRCs of network components are the necessary inputs in a failure estimation algorithm.

These FRCs are used not only to estimate the physical damage to structures but also to estimate the cost of damage restoration [24]. In 1985, the American Applied Technology Group presented a series of seismic risk assessments in California. In this set, multiple functions to assess damage to different types of buildings, facilities, and infrastructure components were developed as matrices of damage. In 1991, in a report titled ATC [25], the association was partially able to compensate for the deficiencies [25]. In 2011, Marano et al. [26] presented a study on two types of concrete structures. In this study, the analytical failure curve was obtained using a random analytical method using data and HAZUS guidance data. In addition, the effect of soil conditions and the impact of structural parameters, such as hardness, elastic hardness ratio to plastic, and structural strength, were also investigated.

Researchers have recently carried out extensive investigations on seismic vulnerability, risk assessment, probabilistic seismic demand analysis (PSDA), multi-hazard risk related to collapse limit state, and improved fragility curve through regression analysis or simulation-based methods. Celik and Ellingwood [27] implemented a reliability analysis-based simulation to determine seismic fragility curves and damage states. Mojiri et al. [28] studied RC models by applying excitation generated by experimental shake tables. Using seismic probability risk assessment and probabilistic seismic demand analysis (PSDA) on experimental data, they determined the seismic demand levels and the corresponding fragility curves. Arabzadeh and Galal [29] investigated the sensitivity and effect

of fiber-reinforced polymer (FRP) retrofitting on the seismic collapse of the system for various tensional effect levels and determined the practical strengthening layout produced by FRP and advanced fragility curves. Faghihmaleki et al. [30] examined a probabilistic framework for the multi-hazard risk associated with the collapse limit state of a G+8 RC moment frame with a shear wall using the Seismostruct software under the blast and seismic loading conditions and generated fragility curves. Huang et al. [31] investigated the probability density evaluation method (PDEM), dynamic reliability, and seismic fragility analysis methods for fragility curve development.

To address earthquake risk reduction, researchers have recently proposed many approaches in the field of vulnerability, including a method to evaluate the seismic risk of urban areas suggested by HAZUS. Another methodology, named the RISK\_UE project, was developed to improve vulnerability assessment in Europe. The main reason for the European Commission's launching of this project was to improve a general seismic risk assessment method in European countries. This came after the realization of the need for a global seismic risk assessment program in Europe, along with other reasons such as the socio-economic and political impact of the seismic events that occurred in Turkey, Athens, Greece, Mouroux, and Le Brun [32]. Two other standard techniques were approved: level 1 (LM1), which is called the vulnerability index-based method (VIM) and was initially developed in Italy [33, 34], and level 2 (LM2), which is named the capacity-spectrum-based method [35]. The vulnerability index method was successfully applied in many European cities, such as Barcelona, Bitola, Bucharest, Catania, Nice, Sofia, and Thessaloniki. Some places where the entire methodology has been tested are Thessaloniki, Greece [36], Barcelona, Spain [37], Mérida, Venezuela [38], Azores, Portugal [39], and Lampedusa Island, Italy [40].

In this study, using nonlinear dynamic analysis in the OpenSees software, we modeled 3-, 5-, and 7-story steel structural frames under the same conditions as in 10 of the earthquake

records near the fault. Incremental dynamic analysis (IDA) was used in the calculation of the FRCs, which are based on the PGA. The parameters in this study are based on drift. In this study, ten earthquake records were split into two clusters, based on whether the earthquake's maximum acceleration was less than or greater than 0.4 g, where g is the acceleration due to gravity. These earthquakes occurred in different parts of the world on soil type II. These records were further split by extracting earthquakes with accelerations ranging from 0.1 g to 1 g at intervals of 0.1 g. Thus, 100 earthquake records were produced. Subsequently, the FRCs for the two-dimensional frames of three steel structures were drawn, which were then investigated and examined by comparing the resulting curves based on the factors affecting the FRCs.

## 2. Methodology

### 2.1. Modeling and selection of earthquake records

In this study, using nonlinear dynamic analysis in the OpenSees software, we modeled three steel structural frames with different stories (3, 5, and 7 stories) under the same conditions as those in 10 earthquake records near the fault. IDA was used in the drawing of the FRCs, which are based on the PGA. The parameters in this study are based on drift values. According to previous studies, using 10 to 20 earthquake records usually yields acceptable accuracy in estimating the damage. Therefore, ten earthquake records extracted from the Pacific Earthquake Engineering Research Center (PEER) earthquake data were split into two clusters (1st and 2nd class), based on their maximum acceleration being less than or greater than 0.4 g. These earthquakes occurred on soil type II. These records were further split into 100 earthquake records by extracting earthquakes ranging from 0.1 g to 1 g at intervals of 0.1 g. The specifications of the 1<sup>st</sup> and 2<sup>nd</sup> class records, the physical properties and seismic properties of the building, and a description of the major column and beam sections are provided in Tables 1 to

**Table 1. Specifications of the selected 1st- and 2nd- class earthquake records**

Class No.	Earthquakes				PGA [m/s <sup>2</sup> ]
	Name	Magnitude	Duration [s]	Year	
1 <sup>st</sup> -records	Imperial Valley (AGR)	6.5	28.430	1979.	0.37
	Imperial Valley (E03)	6.5	11.025	1979.	0.22
	Imperial Valley (CXO)	6.5	39.995	1979.	0.27
	Landers	7.3	49.980	1992.	0.27
	Loma Prieta	6.9	25	1989.	0.3
2 <sup>nd</sup> -records	North Ridge	6.7	29.980	1994.	0.76
	North Ridge	6.7	39.980	1994.	0.85
	Loma Prieta	6.9	39.985	1989.	0.543
	Loma Prieta	6.9	39.990	1989.	0.65
	Tabas	7.4	32.980	1978.	0.4

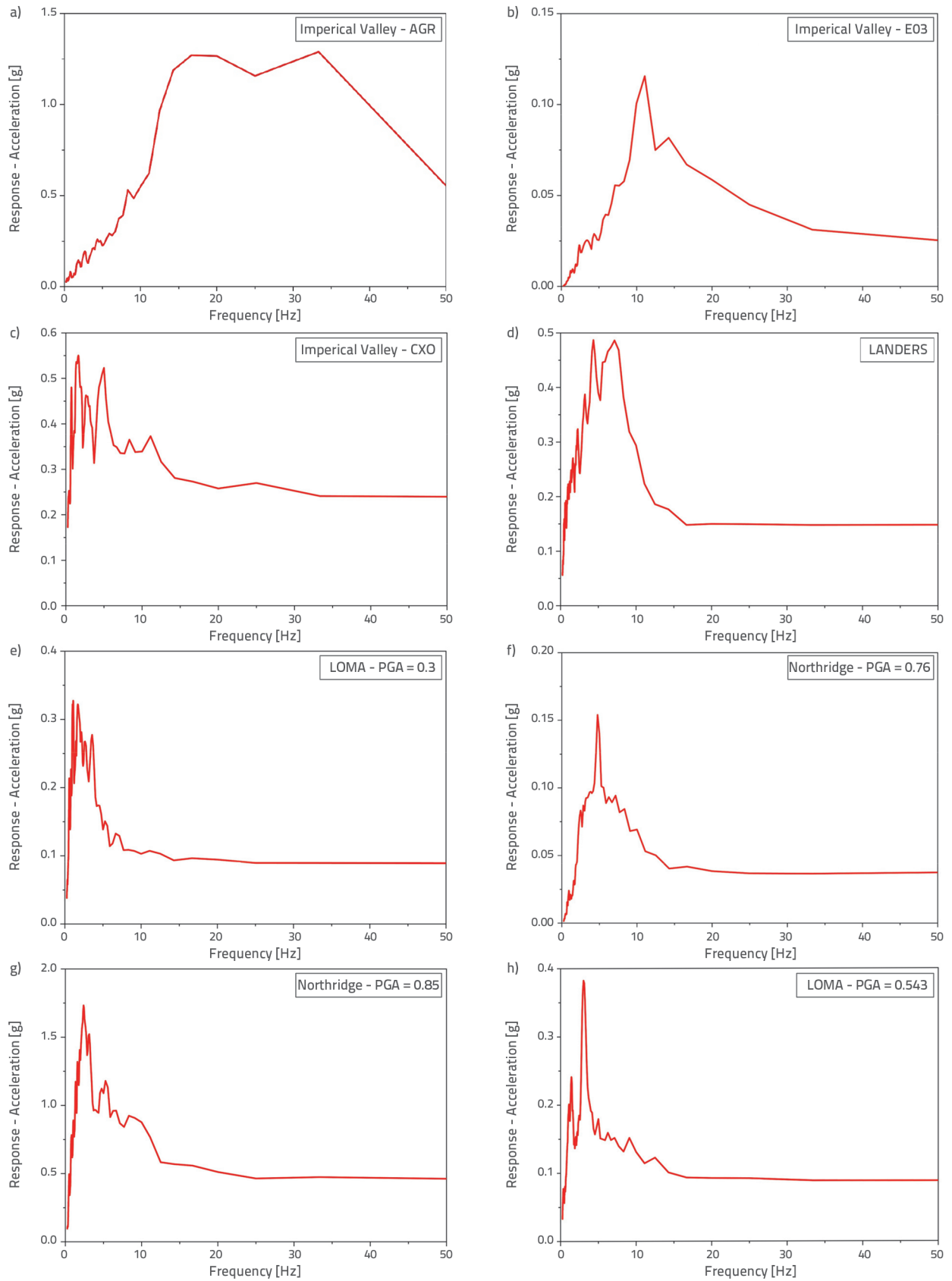


Figure 2. Frequency spectrums of the considered earthquakes, a–e) 1<sup>st</sup> class records, f–j) 2<sup>nd</sup> class records (first part of Figure)

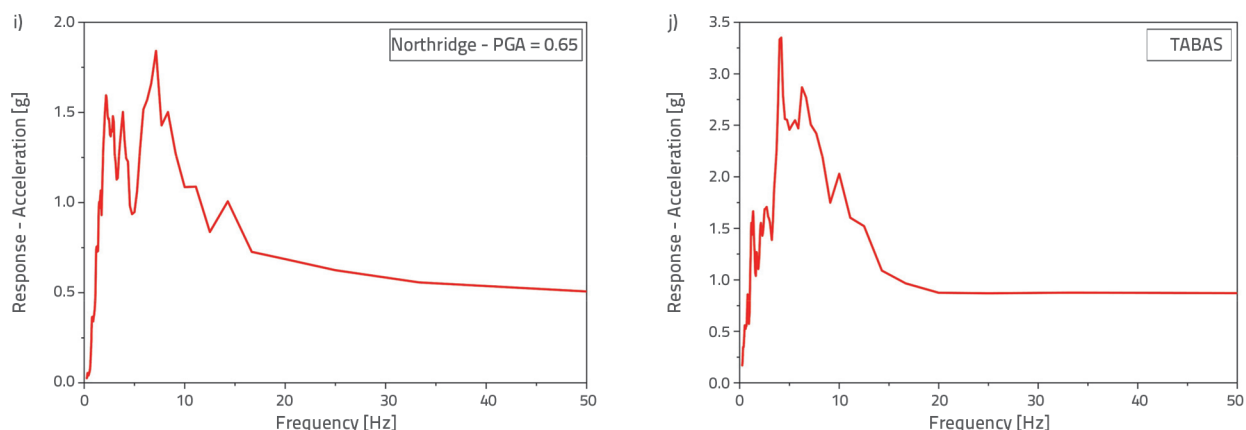


Figure 2. Frequency spectrums of the considered earthquakes, a–e) 1<sup>st</sup> class records, f–g) 2<sup>nd</sup> class records second part of figure)

3, respectively. The isometric and plan view of the 3-, 5-, and 7-story steel frame buildings are shown in Figure 2. All applied loads and soil types were determined with the aid of American Society of Civil Engineers (ASCE) 7/10 design standard (ASCE 2010). Dead loads include the self-weight of beams, columns, slabs, and walls. The thickness of the slab and internal and external walls were considered to be 150 mm, 150 mm, and 200 mm, respectively. Normal weight concrete with a compressive strength of 30 MPa and steel with a yield strength of 360 MPa and elasticity modulus of 200 GPa were used in this study. Rigid diaphragms representing the floor system of the building were created by constraining all points on each floor level in the model. The frequency spectrums of the considered earthquakes have been provided in Figure 3.

Table 2. Properties of models

Parameter	Value
Steel grade	Fe 415
Story height	4.5 and 3.5 m
Total height of building	11.5 m
	18.5 m
	25.5 m
Seismic zone	5
Importance factor (I)	1
Soil type	II
Dead load	4 kN/m <sup>2</sup>
Live load	2 kN/m <sup>2</sup>

Table 3. Major column and beam sections

Model	Story	Story height [m]	Beam and column sections	
			Column	Beam
3 story	1	4.5	W12×87	W24×84
	2	3.5	W12×87	W24×84
	3	3.5	W12×87	W24×84
5 story	1	4.5	W24×146	W27×94
	2	3.5	W24×131	W27×94
	3	3.5	W24×131	W24×84
	4	3.5	W24×117	W24×84
	5	3.5	W24×76	W21×93
7 story	1	4.5	W24×146	W27×102
	2	3.5	W24×146	W27×102
	3	3.5	W24×131	W27×102
	4	3.5	W24×131	W27×94
	5	3.5	W24×131	W27×94
	6	3.5	W24×84	W27×94
		3.5	W24×76	W24×68

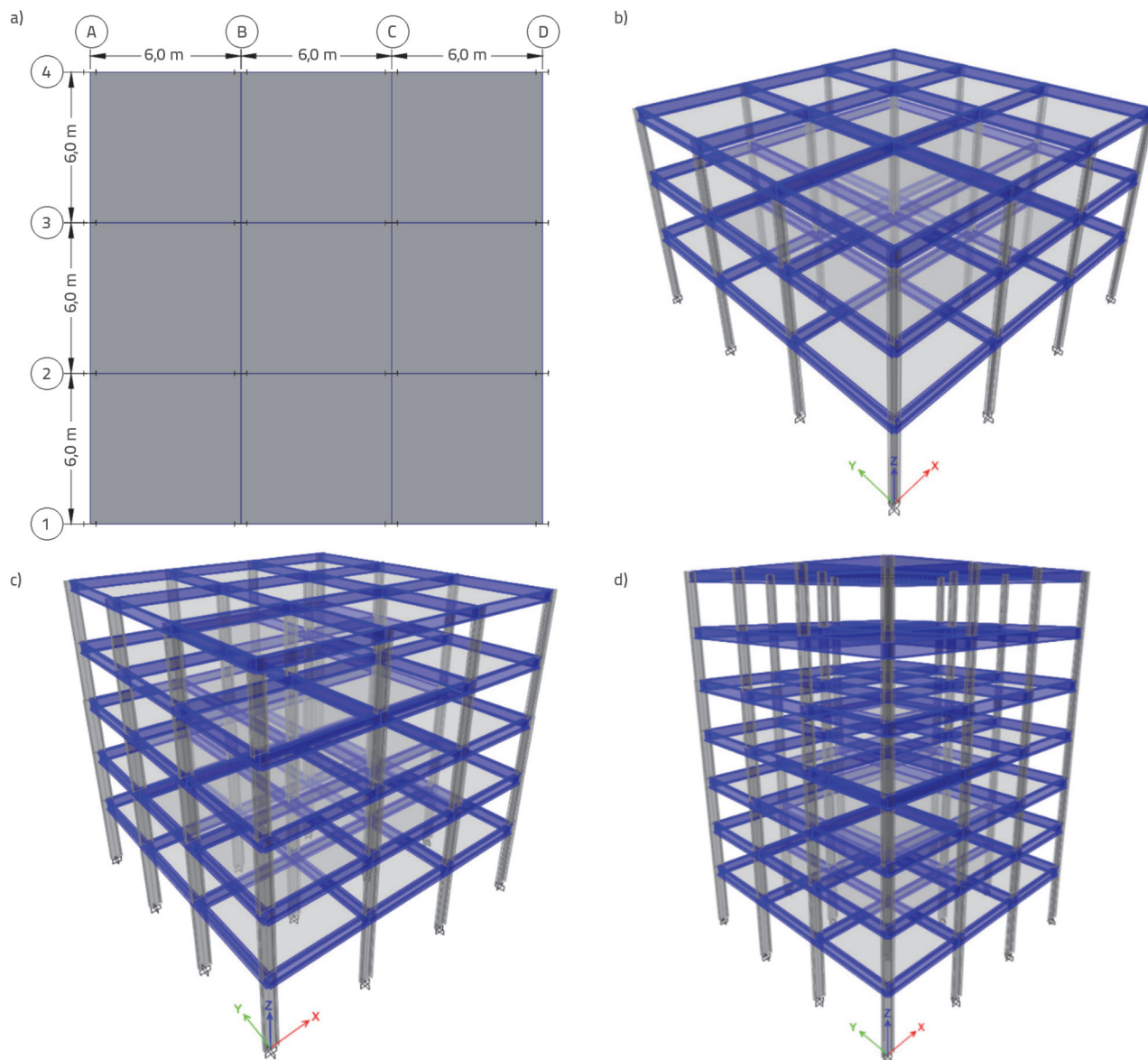


Figure 3. Model views: a) plan view b) 3D view of 3-story, c) 3D view of 5-story; d) 3D view of 7-story

### 2.2. Fragility curves

The fragile seismic curves include two possibilities of independent probabilities. One of these terms is the probabilistic seismic requirement model. The other probabilistic term is more likely to be significant at a certain seismic intensity level than a specific limit of an engineering demand parameter and may be observed at a certain seismic intensity level. The states of the structure are chosen such that they are appropriately reflected in the construction of the design and are included in the structural capacity (C). These possibilities are represented as Eq. (1).

$$\text{fragility} = P[D \geq C | IM] = P[C - D \leq 0,0 | IM] \tag{1}$$

When a seismic level is a requirement, and structural capacity follows a normal log probability distribution, this fragile equation is presented as Eq. (2).

$$P[C - D \leq 0,0 | IM] = \Phi \left[ \frac{\ln \left( \frac{s_d}{s_c} \right)}{\sqrt{\beta_d | IM^2 + \beta_c^2}} \right] \tag{2}$$

where  $\beta_c$ ,  $\beta_d | IM$  and  $s_d$  are the standard deviation of the normal log (dispersion) required in the capacity, the mean of the limit state value or seismic capacity, and the seismic requirement that is a function  $IM - a \cdot \sqrt{\beta_d | IM^2 + \beta_c^2}$  respectively, combined with the HAZUS method and is a  $\beta_{sd}$  parameter. The fragile

relationship is ultimately written as Eq. (3). Figure 4 shows the steps used to develop fragility curves in this study.

$$P_f = \Phi \left[ \frac{\ln \left( \frac{S_d}{S_c} \right)}{\beta_{sd}} \right] \quad (3)$$

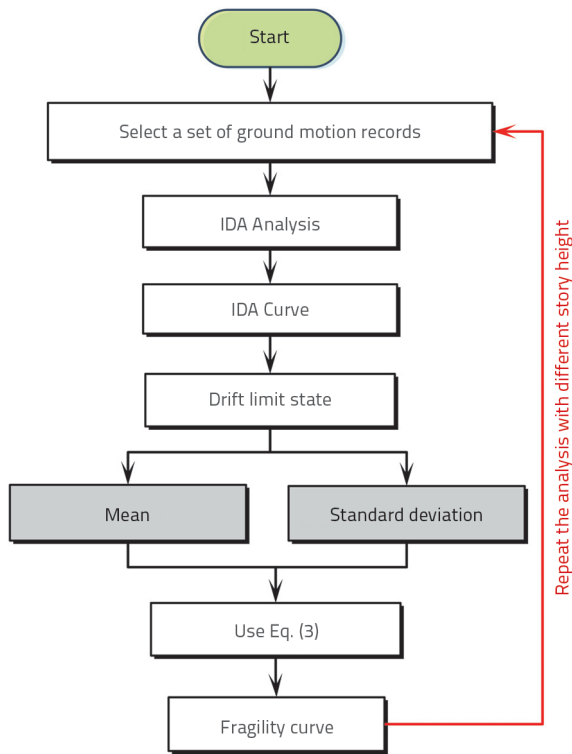


Figure 4. Fragility curve procedure

The damage states introduced in the HAZUS instruction for steel buildings having flexural frame systems with high levels are arranged in the order of partial damage state (slight), medium damage state (moderate), widespread destruction mode (extensive), and state of a complete damage (complete). These four damage states are based on the drift of the middle class. The numerical values for each damage state are presented in Table 4.

Table 4. The drift ratio between two classes for each damage state based on HAZUS

Failure state	Structure with a moderate number of stories	Structure with a large number of stories
Slight (S)	0.004	0.003
Moderate (M)	0.008	0.006
Extensive (E)	0.02	0.015
Complete (C)	0.0533	0.04

### 2.3. Incremental dynamic analysis

One of the most recent methods to represent the FRC is the IDA. In this method, the structural model was subjected to one or more earthquake records and then scaled by altering the intensity levels. After conducting nonlinear dynamic analysis, one or more parametric response curves were calculated at the front of the intensity levels. In these curves, the entire behavioral range of the model is covered. Subsequently, the structure can be evaluated by defining the state of the extent of damage, and the results were expressed as combinations of possible analysis curves, obtained above. After modeling and loading the investigated structures, applying accelerated mapping velocity to the models, and performing an IDA for each model, the maximum amount of drift under the conditions of various earthquake records was obtained, and the obtained values were compared with the criteria defined by HAZUS. Then, using the existing relationships to calculate the probability of failure and the required coefficients, the probabilities of occurrence of the damage states were obtained in any given stock for each model. Finally, the failure curve was plotted using statistical relations between the data. In all graphs (Figures 5 to 7), the horizontal axis represents the maximum lateral displacement (%), and the vertical axis represents the maximum acceleration of the earthquake in terms of acceleration due to gravity. Figures 8–10 represent the results of inter-story drifts for 3, 5, and 7-story buildings for specific earthquakes. The  $S_c$  and  $\beta_{sd}$  values were obtained from the HAZUS instruction for different types of construction and failure and are shown in Table 5.

Table 5. Values of  $S_c$  and  $\beta_{sd}$  (HAZUS instructions)

Type	Slight		Moderate		Extensive		Complete	
	$S_c$	$\beta_{sd}$	$S_c$	$\beta_{sd}$	$S_c$	$\beta_{sd}$	$S_c$	$\beta_{sd}$
S1L	1.3	0.80	2.59	0.76	6.48	0.69	17.28	0.72
S1M	2.16	0.65	4.32	0.66	10.80	0.67	28.80	0.74
S1H	3.37	0.64	6.74	0.64	16.85	0.65	44.93	0.67
C1L	0.9	0.81	1.8	0.84	5.40	0.86	14.40	0.81
C1M	1.5	0.68	3	0.67	9.00	0.68	24.00	0.81
C1H	2.16	0.66	4.32	0.64	12.96	0.67	34.56	0.78

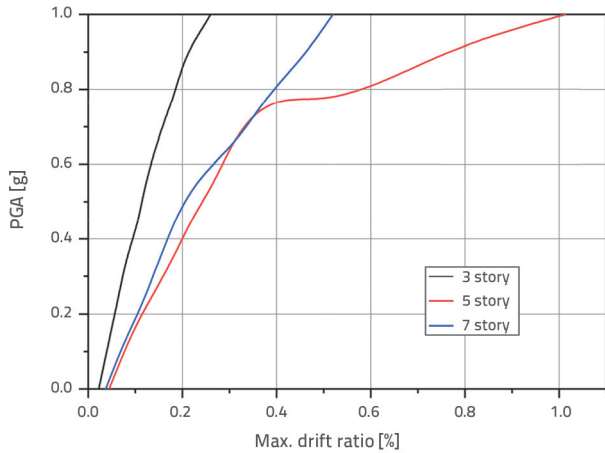


Figure 5. IDA curves for structures with 3, 5, and 7 stories under the Imperial Valley earthquake conditions

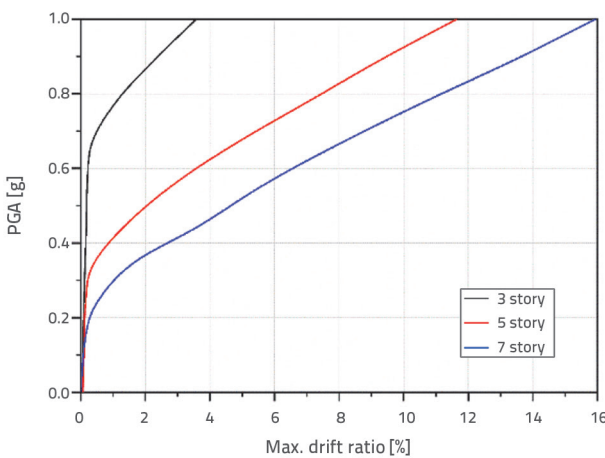


Figure 6. IDA curves for structures with 3, 5, and 7 stories under the Loma Prieta earthquake conditions

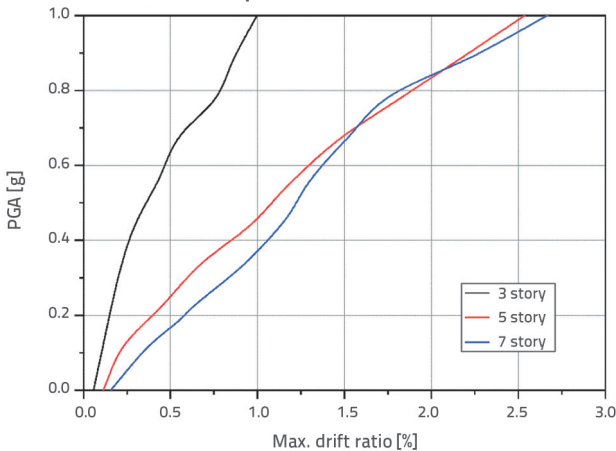


Figure 7. IDA curves for structures with 3, 5, and 7 stories under the Tabas earthquake conditions

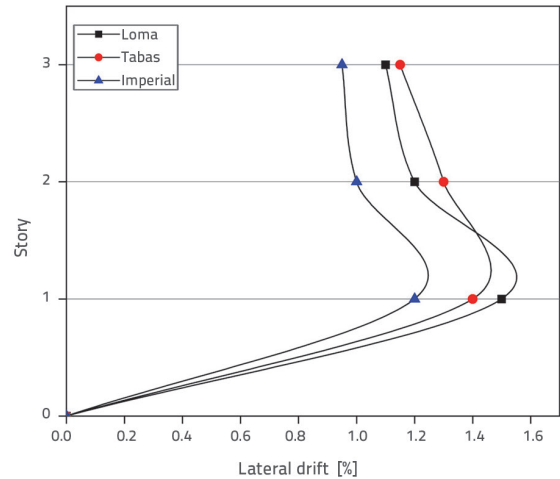


Figure 8. Results of inter-story drifts for the 3-story building

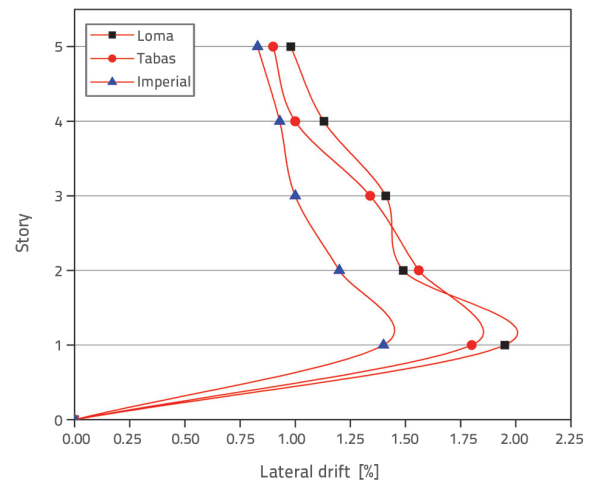


Figure 9. Results of inter-story drifts for the 5-story building

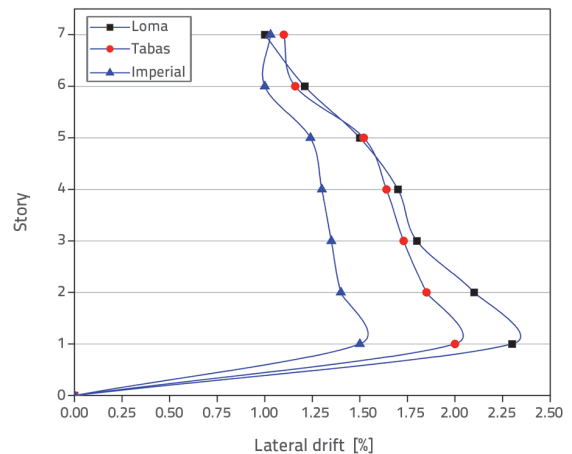


Figure 10. Results of inter-story drifts for the 7-story building

To prepare the diffraction curve using probabilities, the probability of any damage state regarding the number of analyses was determined, and the diffraction curve was generated in terms of Earth's movement probability and intensity. Also, FRCs are presented using the concepts explained

in Eq. (3). These figures are derived from Table 5 for each model and each damage state. By inserting  $\ln(s_d)$ , a numeric value was obtained for each subsequent damage state, and the PGA value was determined by taking the normal distribution of this value. The probability of failure of the structure is described as a

**Table 6. The number of times a structure falls in the four modes of failure under the 1st and 2nd classes of earthquake records**

Records	Slight		Moderate		Extensive		Complete	
	1 <sup>st</sup>	2 <sup>nd</sup>						
3 story	4	4	4	4	1	2	0	2
5 story	3	4	3	3	1	2	1	1
7 story	3	4	4	4	3	3	1	0

combination of probabilities of being at various damage levels. For example, the 5-story structure under the influence of first-class records was found to be in a low damage state five times, in a medium damage state three times, once in a high damage state, and once in a complete damage state.

### 3. Model analysis

For the proper functioning of the structure, the possibility of structural failure at any performance level should be below 50 %; otherwise, the structure’s performance is assessed to be in an undesirable limit state. The FRCs for the 3-story steel model under two different seismic events are shown in Figure 11; for the 5-story steel model in Figure 12, and for the 7-story steel model in Figure 13, respectively. Table 6 lists the number of times a given structure falls in the four modes of failure under the 1<sup>st</sup> and 2<sup>nd</sup> classes of earthquake records. In this study, two different categories of records were used to draw the FRCs. The purpose of this study was to investigate the effect of two classes of earthquake events on the FRCs of steel frames. The main difference between the 1<sup>st</sup>-class and the 2<sup>nd</sup>-class records lies in the maximum ground acceleration. A comparison of the FRCs under the effect of the two different earthquake events is presented in this paper.

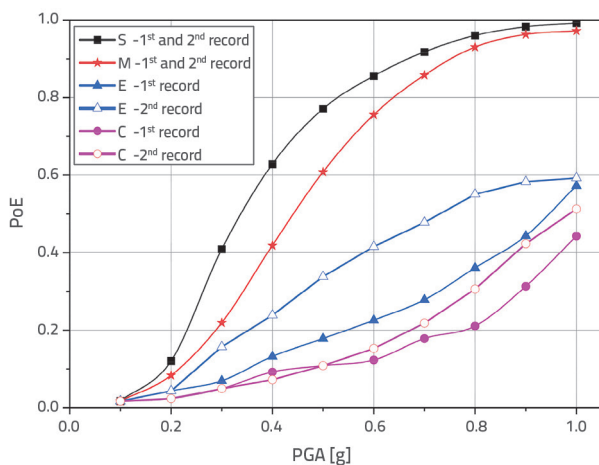


**Figure 11. 3-story structure FRC under the first and second classes of earthquake records**

From Figure 11, it is evident that there is no significant difference in the slight and moderate failure levels of the FRCs under the second class of earthquakes (PGA = 0.85 g) compared to those

under the first class of earthquakes (PGA = 0.35 g). In other words, the increase in PGA has little effect on the probability of exceeding the slight and medium failure levels. The increase in PGA increases the PoE at extensive failure levels for the 3-story structure.

The FRCs under the effect of the second-class earthquake event have significant differences in both slight and moderate failure levels compared to those under the effect of the first-class earthquake event, as seen in Figure 12. In other words, the increase in PGA increased the levels of failure and thus increased the probability of exceeding. The fragility curves for the second category earthquakes shifted from the sleeping mode (gradual increase) to the standing mode (sudden increase) as compared to those for the earthquakes of the first class records. Compared to the 3-story structure, there is a definite increase in the number of times the 5-story structure experiences various modes of failure as the earthquake event changes from the first class to the second class. Consequently, we can conclude that increasing the number of stories increases the probability of exceeding.

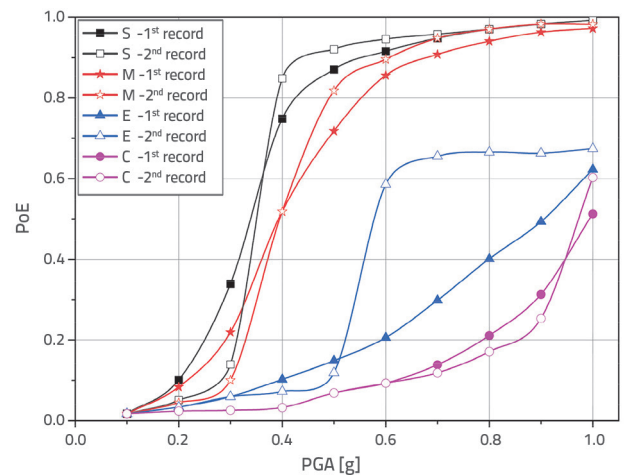


**Figure 12. 5-story structure FRCs under the first and second classes of earthquake records**

The FRCs under the effect of the second-class earthquake event, compared to those under the effect of the first-class earthquake event, show a significant difference at the extensive failure levels, as can be seen in Figure 13. In other words, the increase in PGA increased the probability of exceeding, and in three failure levels (slight, moderate, and high), the PoEs reached 100 %. The

maximum PoE for the complete failure level was 45 % under the first-class earthquake event, and this value increased by 13 % in the case of the second-class earthquake event.

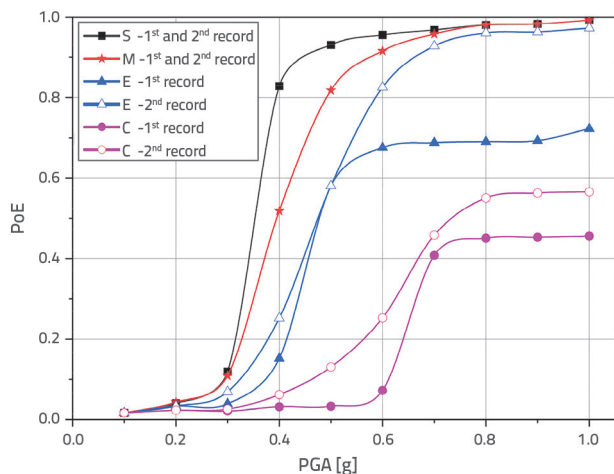


Figure 13. 7-story structure FRCs under first and second-class earthquake records

Finally, the influence of the number of stories on PoE, considering four modes of failure, was investigated. According to Figure 14, increasing the number of stories increases the PoE in extensive and large failure levels. The PoE of the extensive failure mode in the 7-story model was 10 and 15.5 % higher than that in the 5- and 3-story models, respectively. However, for the complete damage state, the PoE in the 5-story model was 6 and 7 % more than in the 7- and 3-story models, respectively. Therefore, it can be concluded that increasing the number of stories increased the PoE, but this increase was more evident for the extensive failure level.

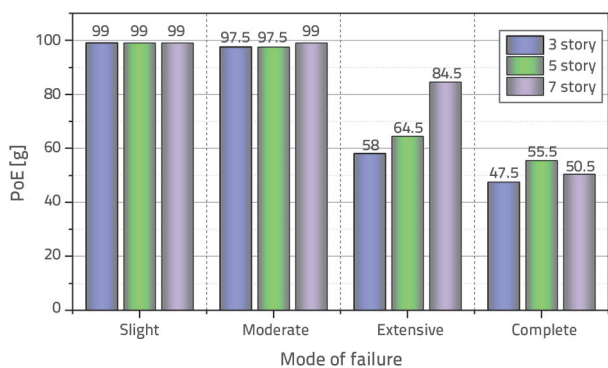


Figure 14. Comparison of PoE in four modes of failure for different number of stories

### 4. Conclusion

The following conclusions can be drawn from our study:

- Increased seismic demand increases the probability of exceeding. In other words, the probability of exceeding (PoE) increases if the maximum earthquake acceleration gets bigger.
- For the 3-story building, there was no remarkable difference in the fragility curves (FRCs) for slight and moderate failure levels under the first or second class earthquakes. However, for the 5-story building, the FRCs under the second class of earthquakes, both the slight and moderate failure levels, had significant differences compared to those under the first class of earthquakes. Moreover, for the 7-story model, the FRCs showed a marked difference compared to those for the 3- and 5-story models at extensive failure levels.
- The PGA increase had little effect on the PoE in the slight and medium failure levels for the 3-story building. However, for the 7-story model, this parameter increased the PoE in three levels (slight, moderate, and high) to 100 %.
- The PGA increase causes an increase in PoE for the 3-story structure at extensive failure levels. The FRCs for the 2nd category earthquakes changed from the sleeping mode (gradual increase) to the standing mode (rapid increase) compared to those for the 1st-class earthquake records for the 5-story model. The maximum PoE of the complete failure level was 45 % under the first class of earthquakes, and this parameter increased by 13 % under the second class of earthquakes.
- Increasing the number of stories increases the PoE in the extensive and large failure modes. The PoE of the extensive failure mode in the 7-story model was 10 and 15.5 % higher than that in the 5- and 3-story models, respectively. However, for the complete damage state, the PoE in the 5-story model was 6 and 7 % more than that in the 7- and 3-story models, respectively. Therefore, it can be concluded that increasing the number of stories increased the PoE, but this increase was more evident for the extensive failure level.

### Acknowledgements

This work was supported by the National Science Foundation of China (Grant No. 51978424).

## REFERENCES

- [1] Sarkhani Benemaran, R., Esmaeili-Falak, M., Katebi, H.: Physical and numerical modelling of pile-stabilised saturated layered slopes, *Proceedings of the Institution of Civil Engineers-Geotechnical Engineering*, (2020), pp. 1-16, <https://doi.org/10.1680/jgeen.20.00152>
- [2] Esmaeili-choobar, N., Esmaeili-falak, M., Roohi-hir, M., Keshtzad, S.: Evaluation of collapsibility potential at Talesh, Iran, *EJGE*, (2013), pp. 2561-2573.
- [3] Galanis, P., Sycheva, A., Mimra, W., Stojadinović, B.: A framework to evaluate the benefit of seismic upgrading, *Earthquake Spectra*, 34 (2018) 2, pp. 527-548, <https://doi.org/10.1193/120316EQS221M>
- [4] Esmaeili-Falak, M., Katebi, H., Javadi, A.A.: Effect of Freezing on Stress-Strain Characteristics of Granular and Cohesive Soils, *Journal of Cold Regions Engineering*, 34 (2020) 2, pp. 05020001, [https://doi.org/10.1061/\(ASCE\)CR.1943-5495.0000205](https://doi.org/10.1061/(ASCE)CR.1943-5495.0000205)
- [5] Esmaeili-Falak, M., Katebi, H., Javadi, A., Rahimi, S.: Experimental investigation of stress and strain characteristics of frozen sandy soils-A case study of Tabriz subway, *Modares Civil Engineering journal*, 17 (2017) 3, pp. 13-23, <http://mcej.modares.ac.ir/article-16-7658-en.html>
- [6] Ghobarah, A., Abou-Elfath, H., Biddah, A.: Response-based damage assessment of structures, *Earthquake engineering structural dynamics*, 28 (1999) 1, pp. 79-104, [https://doi.org/10.1002/\(SICI\)1096-9845\(199901\)28:1<79::AID-EQE805>3.0.CO;2-J](https://doi.org/10.1002/(SICI)1096-9845(199901)28:1<79::AID-EQE805>3.0.CO;2-J)
- [7] Bakun, W.H., Aagaard, B., Dost, B., Ellsworth, W.L., Hardebeck, J.L., Harris, R.A., Michael, A.J.: Implications for prediction and hazard assessment from the 2004 Parkfield earthquake, *Nature*, 437 (2005) 7061, pp. 969-974, <https://doi.org/10.1038/nature04067>
- [8] Güneş, E.M., Altay, G.: Seismic fragility assessment of effectiveness of viscous dampers in R/C buildings under scenario earthquakes, *Structural Safety*, 30 (2008) 5, pp. 461-480, <https://doi.org/10.1016/j.strusafe.2007.06.001>
- [9] Guixin, S.B.Z.: Statistical analysis of the seismic vulnerability of various types of building structures in Wenchuan M8. 0 earthquake [J], *China Civil Engineering Journal*, 5 (2012).
- [10] Padgett, J.E.: Seismic vulnerability assessment of retrofitted bridges using probabilistic methods (Doctoral dissertation, Georgia Institute of Technology), 2007, <http://hdl.handle.net/1853/14469>
- [11] Giordano, N., De Luca, F., Sextos, A.: Analytical fragility curves for masonry school building portfolios in Nepal, *Bulletin of Earthquake Engineering*, pp. 1-30, 2020, <https://doi.org/10.1007/s10518-020-00989-8>
- [12] D'ayala, D., Meslem, A., Vamvatsikos, D., Porter, K., Rossetto, T., Crowley, H., Silva, V.: Guidelines for analytical vulnerability assessment of low/mid-rise Buildings-Methodology. Vulnerability Global Component project, 2014.
- [13] Rossetto, T., Ioannou, I., Grant, D.N., Maqsood, T.: Guidelines for the empirical vulnerability assessment, 2014.
- [14] Benemaran, R.S., Esmaeili-Falak, M.: Optimization of cost and mechanical properties of concrete with admixtures using MARS and PSO, *Computers and Concrete*, 26 (2020) 4, pp. 309-316, <https://doi.org/10.12989/cac.2020.26.4.309>
- [15] Esmaeili Falak, M., Sarkhani Benemaran, R., Seifi, R.: Improvement of the Mechanical and Durability Parameters of Construction Concrete of the Qotursuyi Spa. *Concrete Research*, 13 (2020) 2, pp. 119-134, <https://doi.org/10.22124/JCR.2020.14518.1395>
- [16] Puteri, D.M., Affandi, A.K., Sailah, S., Hudayat, N., Zawawi, M.K.: Analysis of peak ground acceleration (PGA) using the probabilistic seismic hazard analysis (PSHA) method for Bengkulu earthquake of 1900-2017 period, In *Journal of Physics: Conference Series*, 1282 (2019) 1, IOP Publishing.
- [17] Darzi, A., Zolfaghari, M.R., Cauzzi, C., Fäh, D.: An Empirical Ground-Motion Model for Horizontal PGV, PGA, and 5 % Damped Elastic Response Spectra (0.01-10 s) in Iran An Empirical Ground-Motion Model, *Bulletin of the Seismological Society of America*, 109 (2019) 3, pp. 1041-1057, <https://doi.org/10.1785/0120180196>.
- [18] Pan, Y., Agrawal, A.K., Ghosn, M., Alampalli, S.: Seismic fragility of multi-span simply supported steel highway bridges in New York State. II: Fragility analysis, fragility curves, and fragility surfaces, *Journal of Bridge Engineering*, 15 (2010) 5, pp. 462-472, [https://doi.org/10.1061/\(ASCE\)BE.1943-5592.0000055](https://doi.org/10.1061/(ASCE)BE.1943-5592.0000055)
- [19] Wang, Z., Zentner, I., Zio, E.: A Bayesian framework for estimating fragility curves based on seismic damage data and numerical simulations by adaptive neural networks, *Nuclear Engineering and Design*, 338 (2018), pp. 232-246, <https://doi.org/10.1016/j.nucengdes.2018.08.016>
- [20] Singh, S.K., Pérez-Campos, X., Ordaz, M., Iglesias, A., Kostoglodov, V.: Scaling of Peak Ground Displacement with Seismic Moment above the Mexican Subduction Thrust, *Seismological Research Letters*, 91 (2020) 2A, pp. 956-966, <https://doi.org/10.1785/0220190155>
- [21] Kehila, F., Remki, M., Kibboua, A., Bechtoula, H.: Developing seismic fragility curves for existing reinforced concrete structures in Algeria, *Proceedings of the Institution of Civil Engineers-Structures and Buildings*, pp. 1-16, 2020, <https://doi.org/10.1680/jstbu.19.00142>
- [22] Mieses, L.A., López, R.R., Saffar, A.: Development of fragility curves for medium rise reinforced concrete shear wall residential buildings in Puerto Rico, *Mecánica Computacional*, 26 (2007), pp. 2712-2727.
- [23] Caputo, A.C.: A model for probabilistic seismic risk assessment of process plants, In *Pressure Vessels and Piping Conference* (Vol. 50466, p. V008T08A025). American Society of Mechanical Engineers, 2016. <https://doi.org/10.1115/PVP2016-63280>
- [24] Jahangiri, V., Shakib, H.: Seismic risk assessment of buried steel gas pipelines under seismic wave propagation based on fragility analysis, *Bulletin of earthquake engineering*, 16 (2018) 3, pp. 1571-1605, <https://doi.org/10.1007/s10518-017-0260-1>
- [25] Applied Technology Council (ATC): *Seismic Vulnerability and Impacts of Disruption of Lifelines in the Conterminous United States*, 1991.
- [26] Marano, G.C., Greco, R., Morrone, E.: Analytical evaluation of essential facilities fragility curves by using a stochastic approach, *Engineering Structures*, 33 (2011) 1, pp. 191-201, <https://doi.org/10.1016/j.engstruct.2010.10.005>.
- [27] Celik, O.C., Ellingwood, B.R.: Seismic risk assessment of gravity load designed reinforced concrete frames subjected to Mid-America ground motions, *Journal of structural engineering*, 135 (2009) 4, pp. 414-424, [https://doi.org/10.1061/\(ASCE\)0733-9445\(2009\)135:4\(414\)](https://doi.org/10.1061/(ASCE)0733-9445(2009)135:4(414))
- [28] Mojiri, S., El-Dakhkhni, W.W., Tait, M.J.: Seismic fragility evaluation of lightly reinforced concrete-block shear walls for probabilistic risk assessment, *Journal of Structural Engineering*, 141 (2015) 4, pp. 04014116, [https://doi.org/10.1061/\(ASCE\)ST.1943-541X.0001055](https://doi.org/10.1061/(ASCE)ST.1943-541X.0001055)

- [29] Arabzadeh, H., Galal, K.: Seismic collapse risk assessment and FRP retrofitting of RC coupled C-shaped core walls using the FEMA P695 methodology, *Journal of Structural Engineering*, 143 (2017) 9, pp. 04017096, [https://doi.org/10.1061/\(ASCE\)ST.1943-541X.0001820](https://doi.org/10.1061/(ASCE)ST.1943-541X.0001820)
- [30] Faghihmaleki, H., Nejati, F., Mirzagoltabar-Roshan, A., Batebi-Motlagh, Y.: An evaluation of multi-hazard risk subjected to blast and earthquake loads in RC moment frame with shear wall, *Journal of Engineering Science and Technology*, 12 (2017) 3, pp. 636-647.
- [31] Huang, Y., Hu, H., Xiong, M.: Performance-based seismic fragility analysis of retaining walls based on the probability density evolution method, *Structure and Infrastructure Engineering*, 15 (2019) 1, pp. 103-112, <https://doi.org/10.1080/15732479.2018.1520906>
- [32] Mouroux, P., Le Brun, B.: Presentation of RISK-UE project, *Bulletin of Earthquake Engineering*, 4 (2006) 4, pp. 323-339, <https://doi.org/10.1007/s10518-006-9020-3>
- [33] Benedetti, D., Petrini, V.: Sulla vulnerabilità sismica di edifici in muratura: un metodo di valutazione, A method for evaluating the seismic vulnerability of masonry buildings, *L'industria delle Costruzioni*, 149 (1984) 66-74.
- [34] Benedetti, D., Benzoni, G., Parisi, M.A.: Seismic vulnerability and risk evaluation for old urban nuclei, *Earthquake Engineering Structural Dynamics*, 16 (1988) 2, pp. 183-201, <https://doi.org/10.1002/eqe.4290160203>
- [35] Milutinovic, Z.V., Trendafiloski, G.S.: Risk-UE an advanced approach to earthquake risk scenarios with applications to different European towns, Contract: EVK4-CT-2000-00014, WP4: Vulnerability of Current Buildings, pp. 1-111, 2003.
- [36] Kappos, A.J., Panagopoulos, G., Penelis, G.G.: Development of a seismic damage and loss scenario for contemporary and historical buildings in Thessaloniki, Greece. *Soil Dynamics and Earthquake Engineering*, 28 (2008) 10-11, pp. 836-850, <https://doi.org/10.1016/j.soildyn.2007.10.017>
- [37] Lantada, N., Irizarry, J., Barbat, A.H., Goula, X., Roca, A., Susagna, T., Pujades, L. G.: Seismic hazard and risk scenarios for Barcelona, Spain, using the Risk-UE vulnerability index method, *Bulletin of earthquake engineering*, 8 (2010) 2, pp. 201-229, <https://doi.org/10.1007/s10518-009-9148-z>
- [38] Castillo, A., López-Almansa, F., Pujades, L.G.: Seismic risk analysis of urban non-engineered buildings: application to an informal settlement in Mérida, Venezuela, *Natural Hazards*, 59 (2011) 2, pp. 891-916, <https://doi.org/10.1007/s11069-011-9805-9>
- [39] Ferreira, T.M., Maio, R., Vicente, R.: Seismic vulnerability assessment of the old city centre of Horta, Azores: calibration and application of a seismic vulnerability index method, *Bulletin of Earthquake Engineering*, 15 (2017) 7, pp. 2879-2899, <https://doi.org/10.1007/s10518-016-0071-9>
- [40] Cavaleri, L., Di Trapani, F., Ferrotto, M.F.: A new hybrid procedure for the definition of seismic vulnerability in Mediterranean cross-border urban areas, *Natural Hazards*, 86 (2017) 2, pp. 517-541, <https://doi.org/10.1007/s11069-016-2646-9>.